The Feasibility of an Intraneural Auditory Prosthesis Stimulating Electrode Array

Quarterly Progress Report #4

Reporting Period: February 1, 2002 – April 30, 2002

Contract N01-DC-1-2108

Submitted to Neural Prosthesis Program

National Institute for Neurological Disorders and Stroke

National Institute for Deafness and Other Communication Disorders

National Institute of Health

By:

Richard Normann, Ph.D., Principal Investigator

Clough Shelton, M.D., Co-Investigator

Srikantan Najaragan, Ph.D., Co-Investigator

The Center for Neural Interfaces

The Department of Bioengineering

The University of Utah

Salt Lake City, UT 84112

Abstract

The principle activities of the team during this reporting period were focused on 1) preliminary experiments on determining the selectivity of stimulation of the auditory nerve using electrically evoked auditory brain stem response overlap as the index of selectivity, 2) preliminary histological analysis of chronically implanted cat auditory nerves, 3) analysis of frequency maps of auditory cortex resulting from ipsilateral and contralateral acoustic stimulation, and 4) writing (and publishing) a manuscript describing our correlations of MRI estimates of auditory nerve dimensions and cadaveric physical measurements. We have also continued long-term cat implantations to study structural/material biocompatibility. Finally, we have completed the construction of custom stimulators, eABR amplifiers, and signal averagers that are being routinely used in our feline experiments.

1. INTRODUCTION

1.1. PROJECT GOALS

This contract has three specific aims: 1) develop an array of microelectrodes that is suitable for implantation into the auditory nerve, 2) determine the functional potential for this technology to provide a useful sense of hearing, 3) evaluate the risks and benefits of this technology prior to human experimentation. Activities in the first year of this contract concentrate on validating our proposed technique for accessing the auditory nerve, estimating the dimensions of the arrays that can be implanted, and determining the spatial independence of the implanted electrodes. The second year will concentrate on other measures of the functional independence of the electrodes as well as the long-term biocompatibility of the array. The final year of the contract will finish the functional independence studies and center around the chronic electrical stimulation experiments.

1.2. PROGRESS REVIEW TO DATE

1) Surgical Access: We have demonstrated a viable surgical access that allows placement of the Utah Electrode Array (UEA) into the auditory nerve of cats. This has allowed us to use the cat as an experimental animal in our acute and chronic experimentation. We have

also demonstrated a viable surgical access that allows insertion of the UEA into auditory nerve in cadaveric human temporal bones. These accesses should permit insertion of 20 electrodes in a 1.8mm x 2.2 mm array configuration (for 400 micron spaced electrodes), or 80 electrodes in a 200 micron spaced array.

2) eABR Electrophysiological Experiments: We have demonstrated that high velocity implantation of the UEA into the auditory nerve can be accomplished without significant harm to the nerve. This was demonstrated by recording electrically evoked auditory brainstem responses (eABR's) that were evoked by currents injected via a UEA that had been implanted into auditory nerve. Stimulation current thresholds for evoked eABR's have been found to lie in 10μA-50μA range. We were able to record eABR's for up to 48 hours in one acutely implanted cat before the experiment was terminated.

3) Cortical Mapping Experiments: We have demonstrated that we are able to implant UEA's into cat auditory cortex, and that we are able to record single- and multi-unit responses to auditory stimulation. In our most recent work, we have been able to record auditorily evoked single- and multi-unit responses from up to 60-70 of the 100 electrodes in the implanted array.

4) Measurements of auditory nerve dimensions in human cadaveric material: We have measured the diameter of the auditory nerve using MRI measurements and compared these estimates with physical measurements of the same nerves. MRI estimates typically underestimate auditory nerve diameter by 32%.

2. WORK PERFORMED DURING REPORTING PERIOD

2.1. ANIMAL EXPERIMENTS

2.1.1 Stimulation selectivity

One of the motivations underlying this contracted research program was the hypothesis that penetrating electrodes, inserted into the auditory nerve can achieve much more focal stimulation of the auditory nerve than can electrodes on arrays inserted into the cochlea. If this is the case, then it is further postulated that focal stimulation could result in much more selective activation of discrete frequency percepts than could be achieved with cochlear electrodes. One

demonstration of this hypothesis would be to map the various excitation patterns in auditory cortex that are evoked by electrical stimulation of each electrode in UEA's that have been implanted in the auditory nerve, and to demonstrate that stimulation via each electrode evokes an activation map in auditory cortex that does not overlap maps evoked by stimulation of other implanted electrodes. We intend to conduct these mapping experiments in the second year of this program, and we have already performed preliminary experiments where we have demonstrated that we are able to record acoustically evoked responses in cat auditory cortex using UEA's implanted in auditory cortex. However, we have recently conducted a set of preliminary experiments that we feel provides a powerful insight into the issue of selectivity of auditory nerve fiber stimulation.

The experiments are based upon the premise that the amplitude of the electrically evoked auditory brainstem response is proportional to the number of auditory nerve fibers that are activated simultaneously. More specifically (and for the moment, neglecting the issue of auditory nerve fibers that are depolarized by the stimulus but that to not reach threshold for action potential initiation), if we pass current through two electrodes that activate fully overlapping sets of auditory nerve fibers (ie., these are basically identical stimulation sites), the response to the paired stimuli will be no greater than the response to either stimulus delivered by itself. If, however, the two electrodes activate totally independent sets of auditory nerve fibers, then simultaneous stimulation will evoke an auditory brainstem response equal to the sum of each response evoked in isolation.

As mentioned above, there is a caveat to this hypothesis: if we pass current through a single electrode, we will activate a set of auditory nerve fibers located around the tip of the electrode. Further, this current will also depolarize another set of fibers, generally concentrically located around the set of activated fibers, but these fibers will not reach threshold for activation. Simultaneous stimulation via a second electrode inserted in the same site as the first electrode will cause current summation, and the set of fibers that were originally depolarized to a subthreshold level will now be activated and a larger auditory brainstem response will be evoked. This problem can be circumvented by using a sequential stimulation paradigm. If the second stimulus is delayed by 1/3 of a millisecond after the first 0.2 msec long biphasic stimulus, the fibers activated by the first stimulus will be absolutely refractory, and the second stimulus will have no effect on these fibers. Further, the concentrically arranged fibers that have been

depolarized by the first stimulus will repolarize by the time the second stimulus is delivered, and these fibers will not be stimulated by the second stimulus. A number of these hypotheses have been tested in varying degrees in experiments by Miller [1]. We also have conducted a preliminary set of experiments that are described below to directly test these hypotheses.

2.1.1.1 Sequential stimulation with a single electrode.

Figure 1 shows the eABRs evoked by two sequential stimuli delivered via the same electrode. The stimuli were 70 uamps in amplitude, and were biphasic with a 100 microsecond duration per phase (there was no interphase interval). The first stimulus was delivered at 0.05 msec, and the second was delivered at 5.0 msec. The large initial biphasic response to both stimuli is a stimulus artifact. The eABRs evoked by these stimuli follow the stimulus artifacts and can be better seen by rescaling the voltage range on the ordinate. This has been done in figure 2. Here the waves I, II, and III can be easily seen (the pair of 70 uamp stimuli were about 50 uamps above threshold in this experiment). The responses to both stimuli were very similar. This means that the interval between the two stimuli was sufficiently large to allow the fibers excited by the first stimulus to fully recover by the time the second stimulus was delivered (the second stimulus excited these same fibers again).

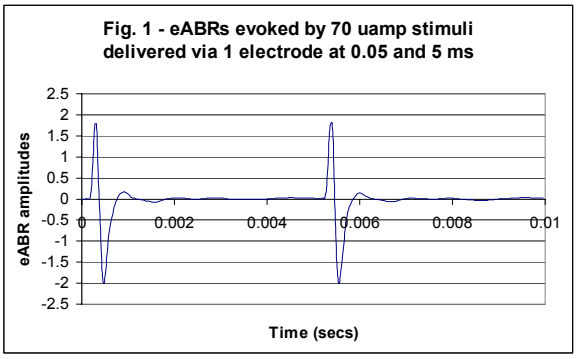

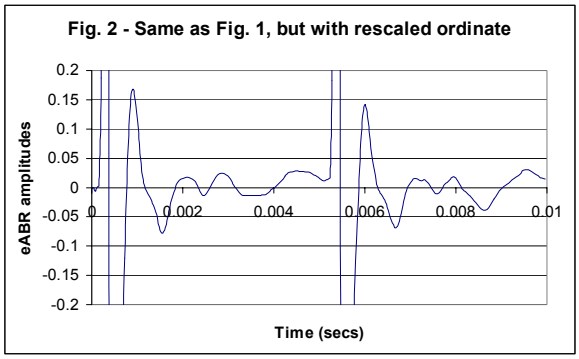

Figure 3 shows the responses that are evoked by passing a pair of 70 microamp stimuli though the same electrode as in figures 1 and 2, but at times 0.05 and 3.0 msec (note that the ordinate has been scaled identically to that used in figure 2). Also note that the response to the stimulus at 3 msec is smaller than that at 0.05 msec. This suggests that all the fibers had not fully recovered from the initial stimulus (delivered at 0.05 msec), and that some fibers are in the 'relatively refractory' state. Figure 4 shows that when the set of responses from figure 3 are subtracted

from those of figure 2, the responses (and the stimulus artifacts) to the stimuli delivered at 0.05 msec almost equal to each other, and almost perfectly cancel out by the subtraction operation. A direct comparison of the responses at 3 msec and 5 msec is difficult to make in this figure, so we have inverted the data from time 0 to 5 msec in figure 5. This allows a more direct comparison between the amplitudes of the responses. It is clear that the response at 3 msec is smaller than that at 5 msec, but both are relatively robust.

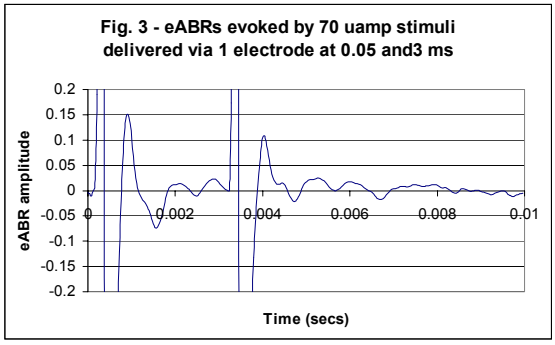

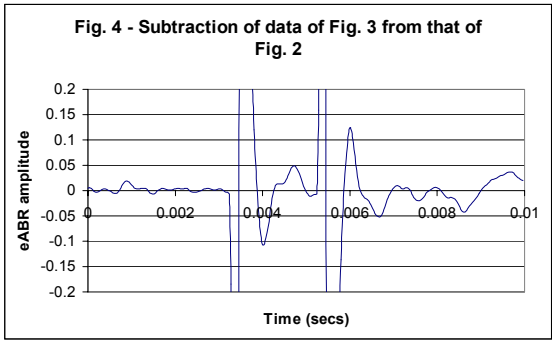

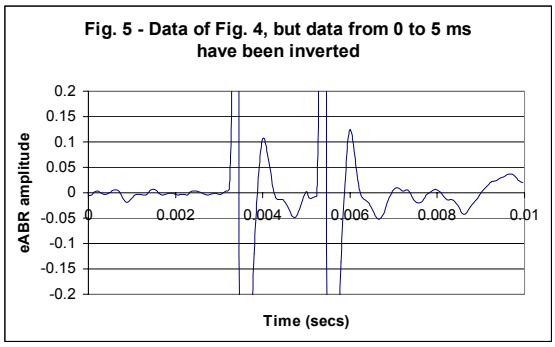

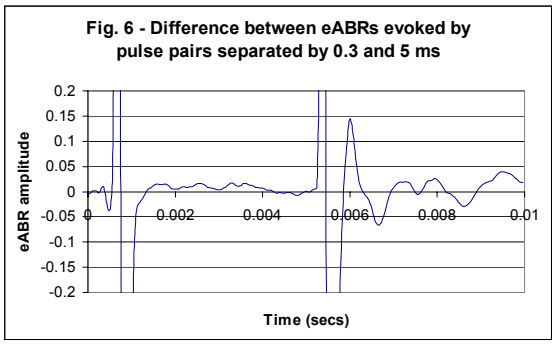

Figure 6 shows the difference between two pairs of stimuli delivered to the same electrode where the first pair of stimuli were delivered at 0.05 and 5.0 msec (the data shown in figure 1), and the second pair of stimuli were delivered at 0.05 and 0.35 msec. It is clear that the fibers stimulated at 0.05 msec are still completely refractory when they are stimulated again, 300 microsecs later.

These experiments, where sequential current pulses were passed via a single electrode demonstrate that 1) a group of auditory nerve fibers excited by a current injection evoke a brainstem response, and are absolutely refractory for at least 300 microseconds, and 2) neighboring, unexcited fibers that experience any subthreshold depolarization produced by this current injection repolarize to their normal resting potential in this 300 microsecond, post-

stimulation interval. The experiments 'set the stage' for estimating the extent of excitation overlap produced by sequential stimulation with pairs of electrodes.

2.1.1.2 Sequential stimulation with two electrodes that excite independent sets of fibers.

In order to estimate the extent of overlap of auditory nerve fibers excited by two electrodes, we have injected current through one of the electrodes, and then after a prescribed interval of time, we have injected an identical amplitude current pulse through the second electrode. If the interpulse interval is short (on the order of 0.3msec), and if there is no overlap between the fibers excited by each electrode, then the response to the second stimulus should be unaffected by the current injection into the first electrode. If there is complete overlap, the second stimulus should evoke no eABR. To quantify the extent of this reduction in the amplitude of the second eABR, we performed this two electrode experiment using two interpulse intervals: 0.3 msecs, and 5.0 msecs. We used the long interpulse interval to quantify the eABR amplitude evoked long after the fiber's refractory periods had ended. The responses to these two interpulse sequences are indicated in figures 7 and 8. In each of these figures, the stimulus artifact produced by stimulation of the electrode stimulated first is smaller than that produced by stimulation by the electrode stimulated second.

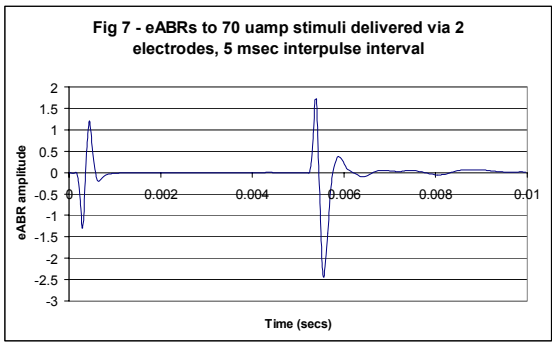

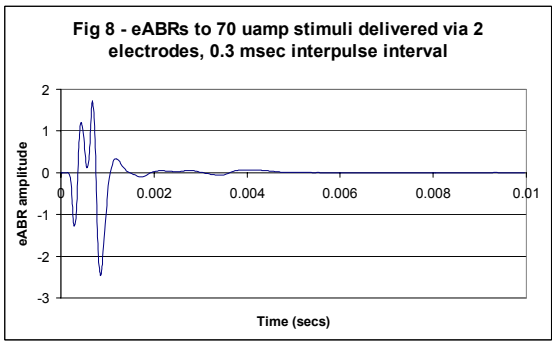

In order to minimize the stimulus artifact produced by the electrode stimulated first, and to permit comparison of the responses evoked by the electrodes stimulated second, we have subtracted the responses of figure 8 from those of figure 7 (and we have inverted the data points from 5msec to 10msec). The subtraction is shown in figure 9, and the eABRs can be better appreciated by rescaling the ordinate (in figure 10).

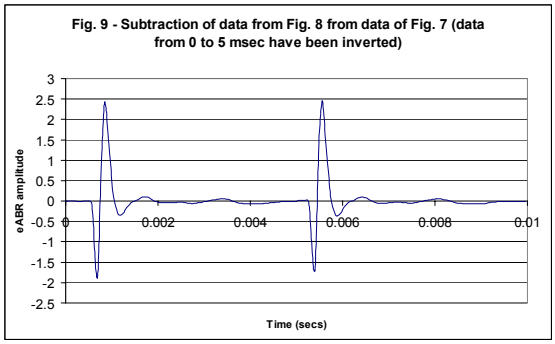

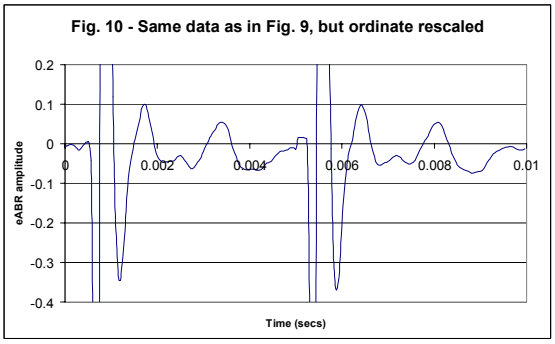

It is clear from figure 10 that the eABR evoked by current injections into electrode 10 (nomenclature used in this particular experiment), delivered 0.3 msec after stimulation via electrode 9, are virtually identical to paired stimulation with a 5 msec interpulse interval. This demonstrates that the sets of auditory nerve fibers accessed by stimulating electrodes 9 and 10 were completely independent. It is also stressed that these results were obtained with current injections of 70 microamps, currents about 50 microamps over eABR thresholds for this experiment. Currents this large were chosen 1) to produce a robust eABR that could easily be extracted from the stimulus artifact, and 2) to recruit a significant number of auditory nerve fibers in order to challenge the sensitivity of the overlap assay we have developed.

2.1.1.3 Sequential stimulation with two electrodes that excite overlapping sets of fibers.

The successful demonstration that this overlap assay can reveal and allow quantification of the extent of overlap between sets of stimulated fibers is further strengthened in other experiments performed in the same animal but in differing electrode pairs. In these experiments, the same paired pulse sequence described in section 2.1.1.2 was used, but in this case, the eABR response to the 0.3msec interpulse interval was considerably attenuated. The subtracted responses (procedure and format identical to those of figures 9 and 10 are shown in figures 11 and 12.

It is clear from figure 12 that for this new pair of UEA electrodes, the eABR evoked after a 0.3msec interpulse interval is substantially reduced and that the kinetics of the response have been eliminated compared to those evoked after a 5msec interpulse interval. We have chosen eABR response data from these two pairs of electrodes in order to illustrate the power of the overlap assay to identify pairs of electrodes with significant overlap and pairs without overlap. We are proposing to conduct additional experiments in the future to quantify the extent of

stimulation overlap between all pairs of electrodes in UEA's that have been inserted into the cat auditory nerve.

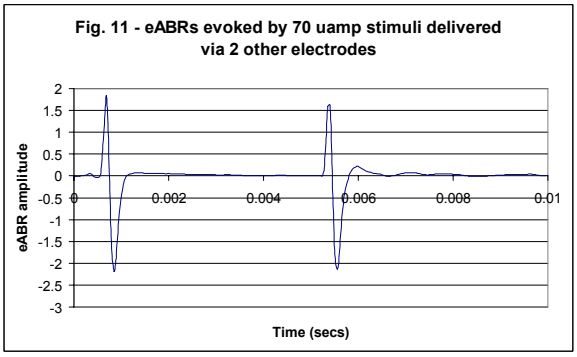

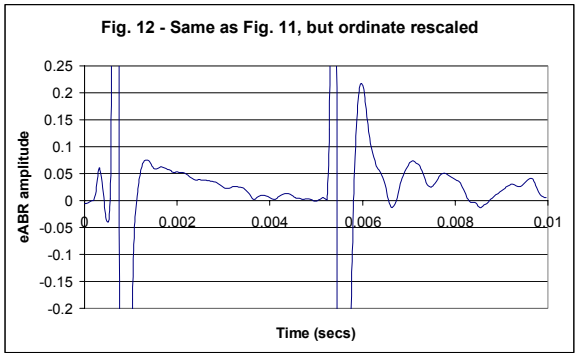

2.1.2 Preliminary histological studies of implanted cat auditory nerve.

Histology of the cochlear nerve and the cat temporal bone is comfounded by the hard temporal bone, and by the presence of hardened bone cement and the brittle Utah Electrode Array implanted into the nerve. We have developed several strategies to overcome these problems.

1. ***Demonstrate that array is in the cochlear nerve:*** We are proposing to decalcify the temporal bone with the array in place and demonstrate in the macro specimen that array is in place. In subsequent decalcified specimens we intend to demonstrate the array position by showing the cochleostomy site with an H&E stain. This will also indicate if bone remodeling in the cochleostomy site tends to push the array out of the nerve.
2. ***Demonstrate the tracks of the array in the nerve:*** We are proposing to harvest the temporal bone and dissect out the nerve inside the temporal bone after explanting the array. Osmium Tetroxide staining of the harvested nerve should demonstrate the array tracks. We may also use H&E stain in these specimens to document any hemorrhage into the nerve.
3. ***Demonstrate effect of implantation on the nerve fibers under Electron Microscopy:*** We intend to fix the cat with 2.5% Glutaraldehyde in 0.1M Sodium Cacodylate Buffer, pH 7.4. This will facilitate EM of the harvested nerve. Specifically, we will demonstrate damage to the fibers near the tip of the array in both active and passive implants. We will use the unimplanted contralateral nerve as the control.

Histological work done till date:

We have done passive implants in total of 13 cats and have let these cat recover and behave freely for varying periods up to 6 months. At the end of implantation periods of 25 days and six months, 2 chronically implanted animals were sacrificed for histology. The animals were deeply anesthetized and perfused with the array in place with formaldehyde acting as a fixative. The array was left in place while the head was immersed in formaldehyde allowing preservation of the electrode implant site in the nerve.

After a week in formaldehyde we removed the array from the nerve and dissected the entire length of the nerve from the temporal bone in one specimen. This tissue was embedded in plastic to facilitate sectioning. Osmium tetroxide stain was used to demonstrate the lipid-rich myelin sheath of nerve fibers.

In an another skull, the temporal bone on either side was harvested and the soft tissues except for the nerves cleaned. The specimens were immersed in a decalcifying reagent, Formical-4 (Decal Chemical Corporation, NY). Formical consists of Formic Acid, Ethylenediaminetetraacetic Acid (EDTA) and Formaldehyde. Our specimens have been immersed in Formical for 21 days and the bone is beginning to decalcify. We hope to be able to provide decalcified images of the bone in weeks to come.

In all specimens, at the time of sacrifice, a visual inspection was performed on the site of implantation and of the explanted UEA. In all cases there was no visual hemorrhage into the implanted site as evidenced by both unaided eye examination of implanted site as well as microscopic examination with 40x magnification. None of the explanted UEAs had any broken electrodes and the microelectrode morphology was undistinguishable from unimplanted UEA under 40x magnification. This indicates that the array did not shatter against the medial side of the modiolus on implantation.

2.1.3 Unit recordings from cat auditory cortex with UEA.

The purpose of these experiments is to demonstrate the feasibility of reliably recording from a large area of cortex using the Utah electrode array (UEA) and to determine the consistency between cortical maps of ipsilateral and contralateral stimuli in AI.

In our previous reports we showed results from preliminary acute experiments in rats and cats, where we recorded simultaneously from multiple neurons in primary auditory cortex (AI) using the UEA. In this report we describe different approaches which we use to analyze data from 10x10 arrays implanted in cat AI.

Experiments described here were performed on acute anesthetized cats with methods similar to those that were described in previous progress reports. A 10x10 UEA was inserted to a depth of approximately 700 microns in AI. Based on 6 successful experiments conducted so far, an average of 69 (+/- 16) electrodes had single or multi unit responses that could be discriminated from the background noise. Eighty-one percent (+/- 14%) of these electrodes responded to acoustic stimuli. Reliable responses were observed within one-hour following implantation and were stable throughout the length of our initial set of experiments (~15-28 hrs). Responses to ipsilateral and contralateral presentations of pure tones of varying intensities and frequencies were recorded and used to determine the characteristic frequency of the neurons.

To determine whether units were responsive to auditory stimuli, we constructed peri-stimulus time histograms (PSTHs) by summing responses to different frequencies and intensities. An example of such a plot is shown in figure 13. A peak in responses following the stimulus indicates the neuron responded to acoustic stimuli.

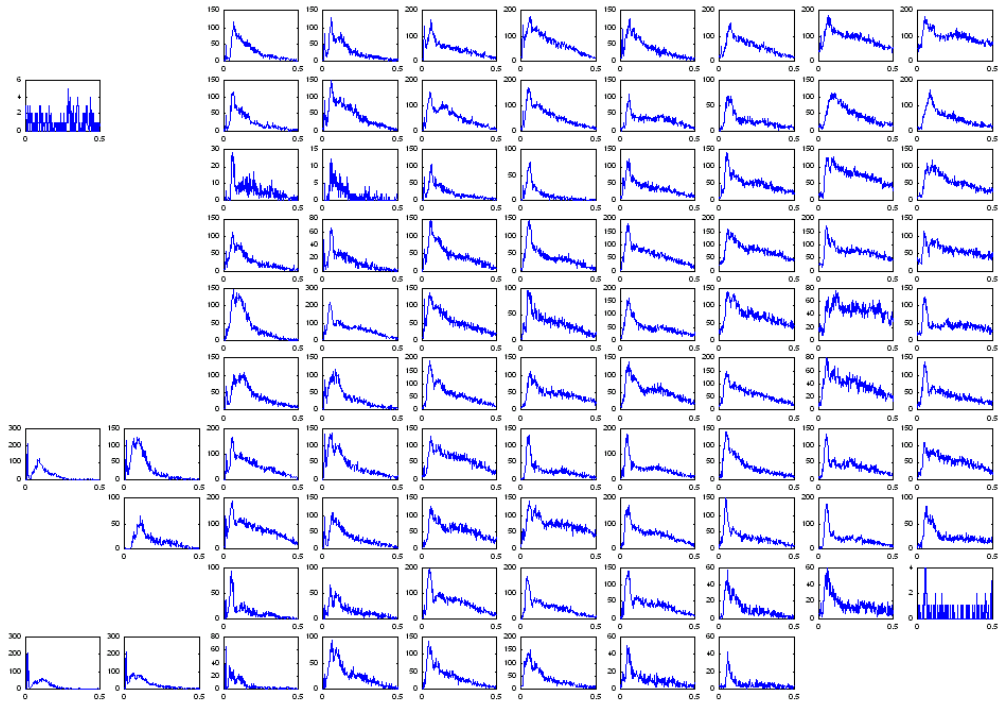

Figure 13: Peri-stimulus time histogram (PSTH) obtained by summing the responses to tones of varying frequencies and intensities. **Note**: geometry of electrodes has been preserved. An absence of a figure panel indicates that no detectable responses were obtained in those electrodes.

Tuning curves were then calculated by counting the number of spikes within a 50 ms. time window following the onset of the stimulus for each presentation. A map of the spike counts for different frequencies and amplitudes (Tuning curve map) is shown in figure 14. To better characterize the responses from electrodes that had multi-unit activity, we sorted the spikes and constructed the tuning curves. We found that response properties were similar for neurons within each electrode for sorted and unsorted data. Tuning curve maps were used to estimate the center frequency (CF) and Threshold for responses in each electrode. A graphical user interface was constructed for the user to select characteristic frequency and threshold of each tuning curve. Some units showed multi peaked tuning. This is consistent with previous literature and can be seen among some electrodes in figure 14.

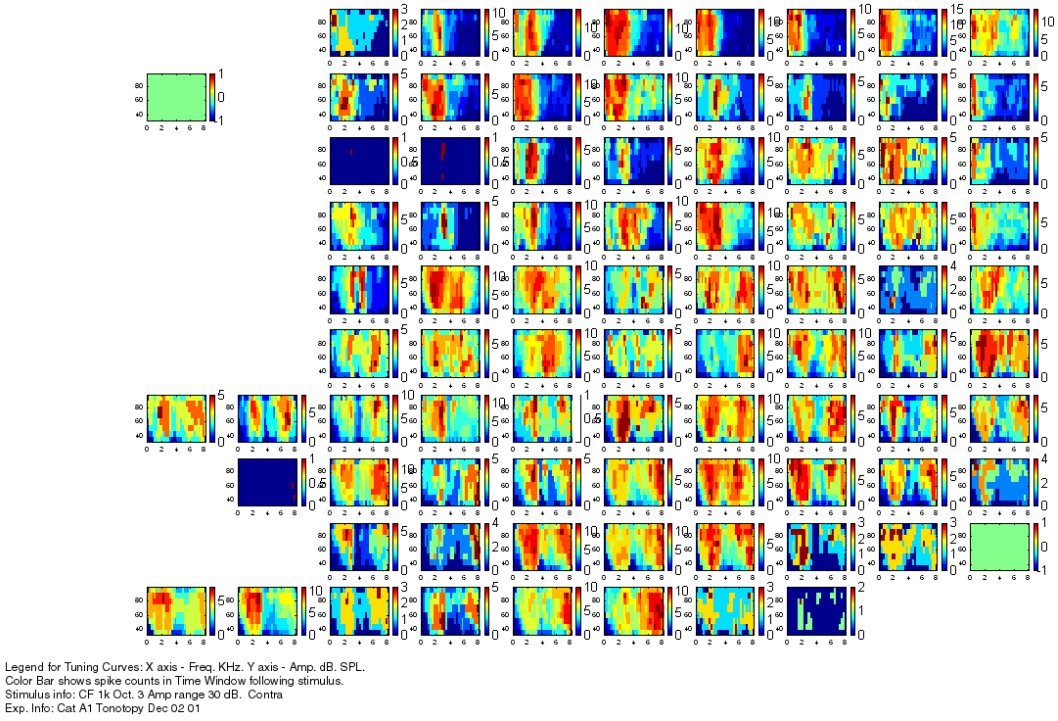

Figure 14: Tuning curve map of responses obtained across the array. The abscissa shows frequency in dB. SPL and the ordinate shows frequency in KHz. The color bar indicates the number of spikes in a 50 ms. time window.

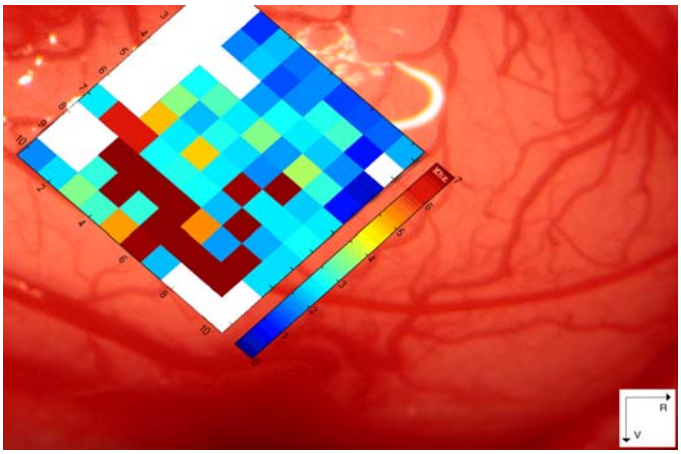

Figure 15: Center frequency map overlaid on the region the array was placed in the cortex. Color bar indicates the Center frequency in KHz. Areas in white indicate that either no response was seen or that no clear center frequency was observed.

The frequency at which the neuron is activated at the lowest amplitude or CF is manually extracted. CFs collected from responses in each channel are shown in a 10x10 grid overlaid on the cortex in figure 15. The center frequencies showed a tonotopic gradient across the array.

Tonotopic gradient reversal was also observed in some experiments indicating that some electrodes in the array recorded from regions adjacent to AI.

Tuning curves appeared to remain stable over the entire recording period. Figure 16 is a plot of CFs extracted from two presentations that were 8 hours apart. A Preponderant data along the diagonal indicated that the CF remained fairly constant over the 8 hr period.

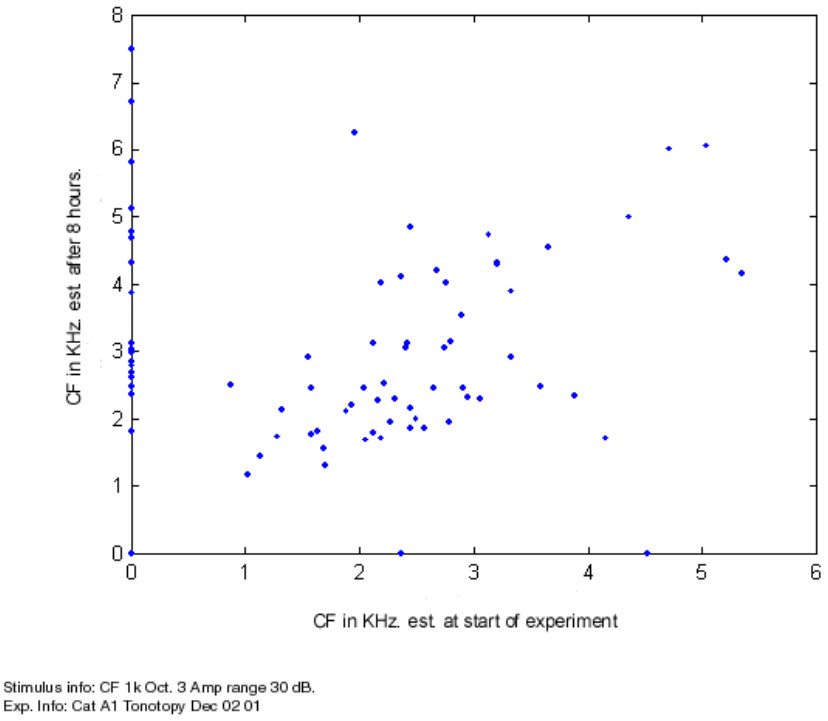

Figure 16: Center frequencies extracted from two similar presentations 8 hours apart. Data points on the ordinate of the plot indicate that neurons were found in channels that were previously inactive.

To compare responses generated by ipsilateral and contralateral stimulation, we plan to use parametric and non-parametric methods. In parametric methods, the CFs and thresholds extracted from tuning curves will be compared for ipsilateral and contralateral stimulation. In non-parametric comparisons, the correlation or mutual information in responses to ipsi- and contralateral stimulation will be calculated. We include some preliminary results from one such analysis in this report.

CFs were extracted from tuning curves generated by ipsilateral and contralateral stimulation. Figure 17 shows a plot of CFs estimated with contralateral acoustic stimulation vs. CFs estimated with ipsilateral acoustic stimulation. Figure 18 shows CFs shown on a 10x10 grid.

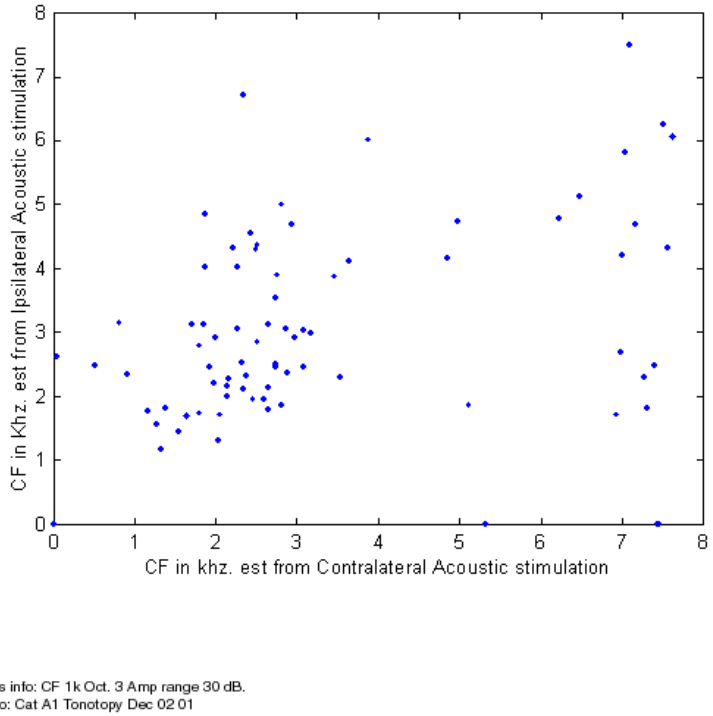

Figure 17: Center frequencies extracted from responses to ipsilateral and contralateral acoustic stimulation.

These preliminary ipsilateral and contralateral response maps show a fair amount of correlation. We are currently exploring different methods of analysis to compare response maps. We are also concerned that there might be some cross talk when stimulating each ear individually. We are planning experiments where we plan to rule out these effects by masking the other ear or even deafening the ear after responses from one side have been obtained.

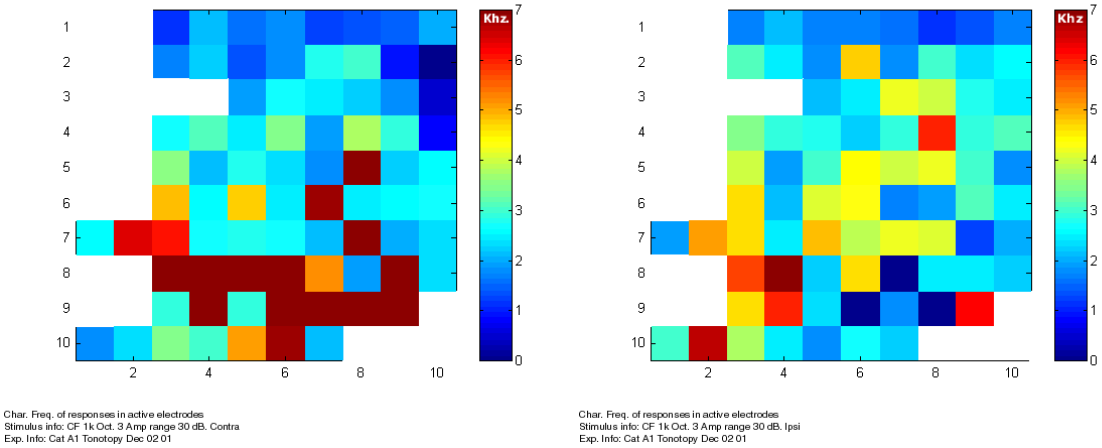

Figure 18: Center frequencies extracted from responses to contralateral (left) and ipsilateral (right) acoustic stimulation. Color bar indicates the Center frequencies in KHz. Areas in white indicate that either no response was seen or that no clear center frequency was observed.

2.1.4 Chronic animal experiments.

A total of 15 animals have been implanted with passive devices during the entire grant period (two of these died during surgery due to anesthesia complications). The remaining 13 have recovered remarkably well given the invasiveness of the surgical access. Two animals have been sacrificed for preliminary histological analysis. The remaining animals will be left for varying periods for up to 6 months before being perfused for histology.

2.2. HUMAN TEMPORAL BONE AND IMAGING STUDIES

It is hoped that the experiments conducted under this research program will uncover and quantify the improvements that direct auditory nerve stimulation can achieve over conventional cochlear electrical stimulation. If this is the case, direct auditory nerve stimulation could provide the 'next generation' auditory prosthesis. However, the optimal insertion of a UEA in a human clinical application will require detailed knowledge of the integrity and size of the cochlear nerve. T2 Fast spin echo magnetic resonance imaging using a FIESTA imaging sequence can give an enhanced view of the nerves of the internal auditory canal by using cerebrospinal fluid as a contrast medium. In order to correlate these findings with direct measurements of the nerve in-situ, we conducted a double-blinded study to detect any significant differences. This component

of the project is summarized in a paper on this subject that was presented by Dr. Tony Owa at the 37th annual meeting of the American Neurotology Society in Florida. This paper has been appended to this report.

We conclude in this paper that MRI scanning tends to underestimate the size of the auditory nerve at the cochlear aperture by 32%, and that this factor varied between specimens. This finding has a major impact on pre-operative decisions regarding the insertion of the intraneural implant. We are not proposing to pursue this component of the research project further at this time.

2.3 INSTRUMENTATION

2.3.1 Portable Stimulator.

Our need for a portable stimulator to be used in the 60 hour electrical stimulation requirement of the contract has motivated us to develop a hybrid digital/analog system with colleagues in Spain. Unfortunately, progress in the development has proceeded slowly due to poor availability of VLSI components. This has caused us to design and fabricate in our Utah laboratory a simple hybrid analog/digital based stimulator. The performance specifications of this stimulator are shown below.

2.3.2 eABR data acquisition system.

In our experiments to date, we have relied upon the use of an ABR data acquisition system that was loaned to us by colleagues in the Otolaryngology Department on an 'as needed' basis. This has proven to be awkward so we have assembled our own system. The system is built in a Labview environment, and consists of an STG 1002 constant current stimulator (Multi Channel Systems), a CP511Grass bioamplifier, and a PCI-MIO-16E-4 data acquisition card (National Instruments) and a Cyber 24 relay board (Cyber Research) to achieve computer controlled switching between electrodes. The performance specifications of the system are listed below, and the system is being used on a regular basis in our feline acute and chronic experimentation.

3. PLANS FOR NEXT REPORTING PERIOD

3.1. ACUTE EXPERIMENTS

3.1.1 Auditory nerve stimulation selectivity

The success we have experienced in our preliminary auditory nerve fiber overlap experiments (described in section 2.1.1) has encouraged us to expand effort in this area over this next quarter. We expect to be able to quantify the degree of stimulation overlap that exists between each electrode in an implanted Utah Electrode Array. The experimentation, analysis and manuscript preparation will likely require significant effort over the next two quarters.

3.1.2 Acute AI mapping.

Our acute mapping experiments will continue. We expect to be able to acutely implant a 12 electrode UEA in the auditory nerve, and by electrical stimulation of the fibers, evoke single unit responses in AI which will be recorded with a 10 x 10 UEA implanted in AI. We will compare ipsilateral acoustically stimulated maps with contralateral electrical stimulation via the UEA implanted in the auditory nerve in order to identify the characteristic acoustic frequency representation of response fields that are activated by stimulation of the auditory nerve via UEAs implanted there. To do this, we must first determine if the characteristic frequency maps evoked by ipsilateral acoustic stimulation are similar to those evoked by contralateral acoustic stimulation. Work which we have begun to study these ipsilateral and contralateral acoustic maps will be continued over the next quarter.

3.2. CHRONIC IMPLANTS

3.2.1. Passive implants.

We have just about completed our passive chronic cat implants over the past quarter, and we have begun conducting histological evaluation of the implanted auditory nerves. Histology will be conducted in the pathology department at the University of Utah, at the pathology laboratory at the VA hospital, and/or by Dr Fred Linthicum, Jr. at House Ear Institute who has agreed to participate in the experiments.

4. PUBLICATIONS AND PRESENTATIONS

The following publications/presentations have been made over this quarter.

Publications

Presentations

A.O.Owa, A.N.Badi, J. Gull, R. Wiggins, T. Hillman, and C. Shelton. Evaluation of the Accuracy of T2 Fast Spin Echo Magnetic Resonance Imaging of the Cochlear Nerve. Presented at the 37th Annual meeting of the American Neurotology Society, held in May 2002 in Boca Raton, Fl**.**

5. DISCUSSION

We are pleased that the preliminary stimulation overlap experiments have proven so successful. These experiments should provide us with a direct determination of the degree of stimulation autonomy of each electrode in an implanted UEA. The subtraction of pairs of eABR records provides a differential technique that minimizes the artifacts due to electrical stimulation. One shortcoming of the technique is the relative small size of the eABR for low stimulation currents (at, or a little above threshold). One would expect that the degree of stimulation overlap would increase with the stimulus strength due to recruitment of larger numbers of auditory nerve fibers. Thus, we would expect to see only minor degrees of overlap with near threshold stimulus levels, but the small eABR responses in this region will make quantification difficult. It is likely that we will have to use larger levels of stimulation where overlap may be more significant.

We also look forward to our histological studies where we can begin to better understand the long and short-term consequences of array implantation into the auditory nerve. The small and gradual increase in eABR thresholds over the period of acute implantation may be due to edema which should be revealed in our histological studies of acutely implanted tissues.

6. LITERATURE CITED

1. Miller, C. A., Abbas, P. J. & Robinson, B. K. Response Properties of the Refractory Auditory Nerve Fiber. *J. of the Assoc. Res. Otolaryngol.* **2**, 216-32 (2001).

Appendix

Evaluation Of The Accuracy Of T2 Fast Spin Echo Magnetic Resonance Imaging Of The Cochlear Nerve

A. O. Owa F.R.C.S. (ORL-HNS) Eng, A.N. Badi M.D.*, J. Gull@, R.Wiggins M.D.#, T. Hillman M.D., C. Shelton M.D. F.A.C.S.
Division of Otolaryngology, Head and Neck Surgery,
University of Utah,
3C120
50 North Medical Drive,
Salt Lake City,
Utah 84132

@Medical student,
University of Utah medical school.

Department of Radiology
University of Utah,
50 North Medical Drive,
Salt Lake City,
Utah 84132

*Centre for Neural Interfaces, Department of Bioengineering, University of Utah, Salt Lake City, UT 84108

This work supported by NIH contract: NO1-DC-1-2108

E-mail- tonyowa@hotmail.com

Address for correspondence:
Clough Shelton M.D., F.A.C.S.
Department of Otolaryngology, Head and Neck Surgery,
3C120 Health Sciences Building,
University of Utah,
50 North Medical Drive,
Salt Lake City,
Utah 84132

Abstract

We have developed a novel intraneural auditory implant-the Utah Slanted Electrode Array, that has the potential of requiring less power and being more frequency-specific than the conventional cochlear implant. The insertion of the device requires detailed knowledge of the integrity and size of the cochlear nerve.
T2 Fast spin echo magnetic resonance imaging using a FIESTA imaging sequence gives an enhanced view of the nerves of the internal auditory canal by using cerebrospinal fluid as a contrast medium. In order to correlate these findings with direct measurements of the nerve in-situ, we conducted a double-blinded study to detect any significant differences.

Method

The ventricular system of cadaveric heads were filled with saline and scanned using a T2 weighted fast spin echo protocol focused on the vestibulocochlear nerves. The vestibulocochlear nerves were then exposed and measured in-situ using an x-y-z stereotactic micrometer. Measurements of the nerve width were made at the cochlear aperture and these were compared with the MRI measurements.
Both the radiologist and the dissector were unaware of each other's measurements at the time of the study.

Results

Four specimens were obtained, but one was discarded, as we were unable to keep fluid within the ventricular system. A total of six cochlear nerves were dissected. Direct measurements ranged from 1.16-1.33mm compared to 0.65-1.1mm with MRI measurements. The average nerve diameters 1.27mm (direct measurements) compared to 0.83mm (MRI). Statistical analysis showed a significant difference, however, a correction factor of 32% was found.

Conclusion

MRI scanning tends to underestimate the size of the auditory nerve at the cochlear aperture by 32%. This would have a major influence on pre-operative decisions regarding the insertion of the intraneural implant.

Keywords: Auditory nerve implant, Cochlear implantation, MRI scanning, Cochlear nerve.

Introduction

Cochlear implants have revolutionised the management of profoundly deaf patients. Increasing number of implanted children are being educated in mainstream schools with immense financial and social benefits. Cochlear implant companies are presently trying to develop smaller devices with better speech discrimination. One such strategy is by trying to place the electrodes closer to the modiolus (Nelson et al). But these attempts cannot overcome the problem of stimulation through the intervening modiolar bone leading to less focal stimulation at higher currents. The development of the Utah Electrode Array (UEA), an array of penetrating intraneural microelectrodes promises to eliminate these inherent disadvantages of the present cochlear implant devices.

The basic UEA is a micro machined array of 1 mm long silicon-based electrode needles that project out from a common 0.2mm thick silicon substrate. Each electrode is insulated with polyimide or silicon nitride. Glass is used to electrically isolate the electrodes from each other at the base. The array is then connected to a percutaneous connector by platinum iridium wires. Only 25μm of the tip of these electrodes is deinsulated, providing for stimulation of very discrete bundles of fibers in a nerve. A slight modification of this array is the Utah Slant Array (USA) (Figure 1). This array has electrodes of varying lengths to facilitate different depths of penetration to take advantage of the tonotopic arrangement of the nerves (2), (3). Direct implantation of the electrode in the cochlear nerve should result in very focal stimulation with reduced power requirement of the device and hence may be the first step in the development of a totally implantable device. It is also expected to recruit more frequencies compared to the conventional cochlear implant because of the placement of the electrodes in the nerves. Patients with intact cochlear nerves but abnormal or unsuitable cochleas would benefit from the device.

The main concern with the device is that it needs to be custom made for each nerve hence an accurate preoperative assessment of the cochlear nerve dimensions is imperative. At the present time MRI scans provides the most accurate means of evaluating the size of the nerves of the internal auditory canal. Even though measurements have been made regarding the size of tumours affecting these nerves based on computer-assisted calculations, they have been shown to be inaccurate on a number of occasions (4-10). There also appears to have not been any study to compare the estimated size of the nerves with actual cadaveric or human measurements.

This study aims to identify any disparity between cadaveric and MRI measurements and if there is to try and see if there a correction factor can be determined to aid assessments.

Method

Four cadaveric heads were obtained. In order to mimic the contrast properties of C.S.F., saline was instilled in to the ventricular system of the cadaveric heads. The head were then imaged using the fast imaging employing steady state acquisition (FIESTA) protocol in with fluids give a bright signal on imaging. The neuroradiologist then measured the diameter of the cochlear nerve at the cochlear aperture (Figure 2).

All imaging was obtained on a GE LX CV/i 1.5 Tesla MRI (GE Medical Systems, Milwaukee, WI). A 3'dual-phased array surface coil was utilized for both sequences. The T2 weighted images were acquired with the routine protocol for High-Resolution Fast-Spin Echo (FSE) MRI, at the University of Utah. This was performed with acquisition of a 3D FSE volumetric data set with the following parameters: TR 4000, TE 130, 256 X 256 matrix, 13cm FOV, 1 NEX, echo train length: 64, with 30, 0.8mm sections being acquired in a slab, with a total acquisition time of 8 minutes. These were then reconstructed in an oblique sagittal plane, perpendicular to the long axis of the IAC, in 1mm thick sections with no intersection gap. The Fast Imaging Employing Steady-state Acquisition (FIESTA) images were also obtained with the 3' dual-phased array surface coils. A similar 3D volumetric data set was acquired with the following parameters: TR 8, TE 4, 256 X 256 matrix, 10cm FOV, 6 NEX, with 32, 2mm sections being acquired in a slab, with a total acquisition time of 6:30 minutes. These were then similarly reformatted in an oblique sagittal plane, in 1mm thick sections, with no intersection gap.

The cochlear nerves were subsequently dissected out using an extended translabyrinthine approach to expose the entire cochlear nerve. In-situ measurements were taken at a point corresponding to the location of the neuroradiologist's measurements. The radiologist and the surgical dissector were blinded to each other's measurements. The length and thickness of the exposed nerves were measured with a World Precision Instruments (WPI) tungsten microelectrode (World Precision Instruments, Sarasota FL) having shaft diameter of 0.254 mm and a tip diameter of 1-2 μm, positioned with a X Y Z axis calibrated micromanipulator on a stereotaxic frame (Figure 3). We used a Kopf Model 1761 micromanipulator (David Kopf Instruments, Tujunga, CA) that has three screw-driven slides with 10μm resolution each, plus a universal joint for measuring angles. The tip of the electrode was positioned over the nerves and viewed under x40 operating microscope. The manipulator and the operating microscope was positioned parallel to the length of the nerve to avoid parallax. Position of the manipulator was further confirmed to be parallel to the exposed nerve and the Z-axis, the axis of the depth of the nerve, was normalized by adjusting the angle and depth of measurement for the entire length of the nerve. The dimensions of the cochlear nerve at the cochlear aperture were measured at a point, which corresponded with the radiological location of the cochlear aperture.

All the investigators were blinded to the results of the measurements. The results were subsequently analysed for statistical differences at 95% confidence limits using paired t-test.

Results

One head was excluded from the analysis because we were unable to fill the ventricular system with fluid. . A total of six cochlear nerves were dissected. Direct measurements ranged from 1.06-1.5mm compared to 0.69-1.15mm with MRI measurements. The average nerve diameters 1.27mm (direct measurements) compared to 0.83mm (MRI). Statistical analysis using student t test showed a significant difference between the two sets of measurements. However, after a correction factor of 32% was applied to the FIESTA MRI measurements there was no statistical difference between the two sets.
A summary of the result is illustrated in table 1

Discussion

MRI are increasingly being used in planning the management of a large range of conditions. Improved imaging techniques and machines are leading to the development of better, faster and ultimately less expensive protocols. The FIESTA (Fast imaging employing steady state acquisition) imaging sequence is an MRI pulse sequence designed to significantly increase the signal to noise ratio in a very short amount of time. This type of pulse sequencing accentuates the contrast of fluid, while relatively suppressing signal from soft tissues, and is therefore useful for imaging clinical applications that benefit from this application. Examples of such indications include cardiac muscle, bile ducts, and IAC imaging. General benefits of the FIESTA technique include excellent signal-to-noise ratio, decreased scan times, improved contrast resolution between fluids and soft tissues, and improved flow compensation, which can significantly degrade some MRI series, such as blood flow artefacts.

The evaluation of the IAC and cranial nerves is a specific area of advantage of the FIESTA technique compared with more traditional MRI sequences. Specifically comparing this technique with 3D-FSE T2 weighted imaging (often used for high-resolution IAC imaging), FIESTA offers decreased CSF pulsation artefacts, improved contrast to surrounding anatomic structures, approximately 50% decrease in overall scanning time with similar voxel size and field of view (FOV) settings, and the ability to take advantage of gadolinium contrast enhancement of lesions within the IAC. Some of the obvious disadvantages of FIESTA compared to conventional 3D-FSE T2 weighted imaging include the requirement of increased gradient abilities of an MRI scanner, increased magnetic susceptibility (artefacts from metal) and heterogeneous signal from blood vessels, making this sequence a poor choice for vascular evaluation.

While MR imaging have improved our diagnostic ability especially in detecting abnormalities of the vestibulocochlear nerves, this study highlights some of the findings in clinical practice where radiological measurements are found not to concur with operative findings (4). Shelton et al (5) reported a subset of profoundly deafened patients with radiological evidence of a narrow auditory canal that responded poorly to cochlear implantation. Gray et al (6) and Maxwell et al (7) also reported similar experiences. In contradistinction to this Bamiou et al (8,9) reported on two patients with radiologically absent cochlear nerve who had Audiological responses. The scans used were a CT scan of the petrous bones and internal auditory meatuses using a Siemens Somaton +4 scanner in 1mm serial axial and coronal cuts. Axial scans were oriented parallel to the infra-orbital - meatal line, while coronal scans were tilted at 105° angle to this line. MRI scans were focussed on the inner ear, internal auditory meatuses (IAM) and cerebellopontine

angle and were performed on a Siemens vision 1.5 Tesla scanner in 1mm serial axial and coronal cuts except for case 10, whose MRI was done in 3mm cuts. They suggested that these findings were due to inadequate resolution of the scanning machines, which they believe were unable to discern nerve sizes less than 3mm. Ackers et al (10) also reported on a child with a good response to cochlear implantation despite having absent or hypoplastic cochlear nerves on imaging.

These discrepancies would certainly need to be taken into account during surgical procedures dependent upon an accurate assessment of the dimensions of lesions or tissues being implanted. The Utah array is an array of 1mm long silicon-based electrode needles that project from a 0.2mm silicon substrate. The Utah slant array allows for three-dimensional stimulation and recording potential. The array can be manufactured with electrode of progressive length, allowing for nerve implantation at different depths. The small size of the array with compact electrode spacing could also allow for 200 individual electrodes to be placed in the cochlear nerve. The size and number of electrode to be implanted would depend on the size of the cochlear nerve of the patient. We propose to implant the array using a modified extended facial recess approach. We have been able to demonstrate this approach in acute animal and in cadaveric specimen (11).

Although the sample size is small, the results are statistically significant as the differences are in the same direction and the variability was small. In addition the correlation between the two measurements was not statistically significant. In the absence of any population statistics an assumption of a clinically significant effect can be considered to be 2mm. This would suggest a variance of 0.33 with the power of the study being 90% despite the small sample size. However, the relatively large correction factor is not commonly seen in clinical practice even though some discrepancies have been observed. This may be due to a variety of reasons one of which could be due to the small dimensions of the cadaveric nerve in this study and whilst the numbers of nerves dissected out reached statistical significance this may not necessarily be the case clinical practice. One may also surmise that there may have been calibration problems with the new imaging protocol or indeed the measurements were not made at corresponding points however these discrepancies would have interfered with the determination of a correction factor. The possibility that the discrepancy could have been due to the resolution of the scanning machine not being accurate enough has already been alluded to. There is certainly scope for further studies to resolve this issue. The use of the FIESTA MRI sequence utilising a correction factor allows a fairly accurate determination of cochlear nerve dimensions. This will allow preoperative selection of the proper sized cochlear nerve electrode array and facilitate placement of the maximum number of penetrating electrodes.

Conclusion

This study shows that MRI consistently underestimates the size of the cochlear nerve by 32%. This correction factor should be considered when planning surgery. This has a direct bearing on the newly developed intraneural device where an accurate assessment of the nerve dimension preoperatively is of immense importance to the outcome.

References

1) Nelson D.A., Van Tassell D.J., Schroder A.C., et al Electrode ranking of "place pitch" and speech recognition in electrical hearing. J. Acoustic Society of America 1995; 98(4): 1987-1999.

2) Lorentente de No R. The sensory endings in the cochlea. Laryngoscope 1937; 47: 373-377.

3) Sando I. The anatomical interrelationships of the cochlear nerve fibers. Acta Otolaryngologica. 1972; 76 (1): 1-20.

4) Selesnick SS, Rebol , Heier LA, Wise JB, Guttin PH, et al . Internal auditory canal involvement of acoustic neuromas: Surgical correlates to Magnetic resonanace imaging findings. Otology & Neurotology 2001; 22: 912- 916.

5) Shelton C., Luxford W.M., Tonokawa L.L., et al The narrow internal auditory canal in children: a contraindication to cochlear implants. Otolaryngology, Head and Neck Surgery. 1998; 100:227-231.

6) R.F. Gray, Ray J., Baguley D.M., et al. Cochlear implant failure due to unexpected absent eighth- a cautionary tale. Journal of Laryngology, Otolaryngology. 1998; 112: 646- 649.

7) Maxwell A.P., Mason S.M., O'Donoghue G.M. Cochlear nerve aplasia: its importance in cochlear implantation. American Journal of Otology. 1999; 20: 335-337.

8) Bamiou D.E., Omahoney C., Sirimanna T., Useful hearing despite radiological findings suggestive of anacusis. J Laryngology and Otology 1999; 113:714-16.

9) Bamiou D.E. Worth S., Phelps P., Sirimanna T., Rajput K., 2001 Eight nerve aplasia and hypoplasia in cochlear nerve patients Clinical Perspective Otology and Neuro-otology; 22: 492-496.

10) Acker T, Mathur NN, Savy L, Graham JM. Is there a functioning vestibulocochlear nerve? Cochlear implantation in a child with symmetrical auditory findings but asymmetric imaging. Int J Pediatr Otorhinolaryngol 2001; 57(2): 171-6.

11) Badi A.N., T. Owa, Shelton C., Normann R.A., "Novel Auditory Prostheses Using an Intraneural Stimulating Electrode Array", 32nd Neural Prosthesis Workshop, 2001, NIH, Bethesda, MD.

Figures and Figure Legends

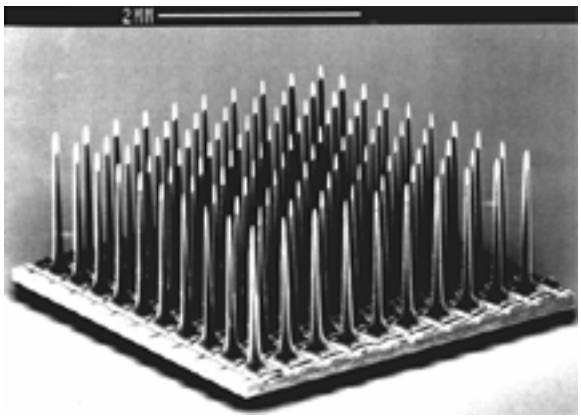

Figure 1. Utah eletrode array. It consists of 1mm silicon based electrodes needles that project from a common 0.2mm thick silicon substrate. Each electrode is insulated with polyimide or silicon nitride and electrically isolated from each other with glass. The tip is deinsulated allowing it to stimulate discrete areas of the nerve. The array is connected to a percutaneous connector using platinum iridium wires.

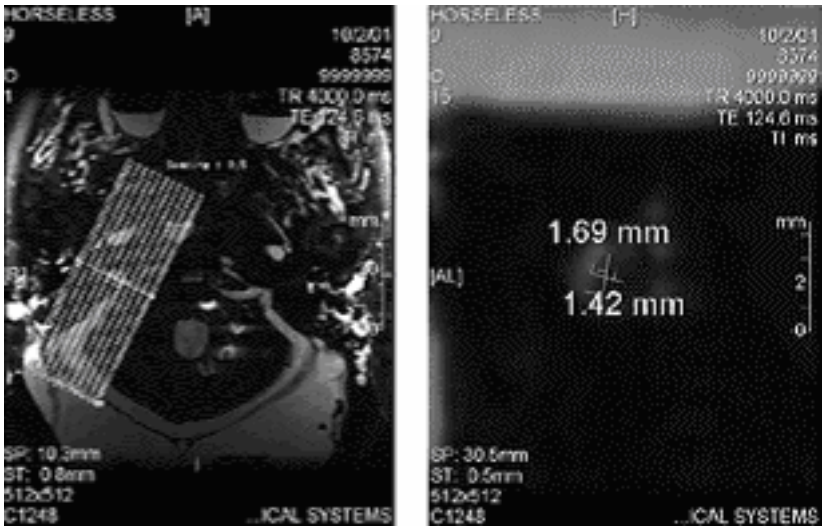

Figure 2 MRI saggital section of the internal auditory meatus using the FIESTA sequence.

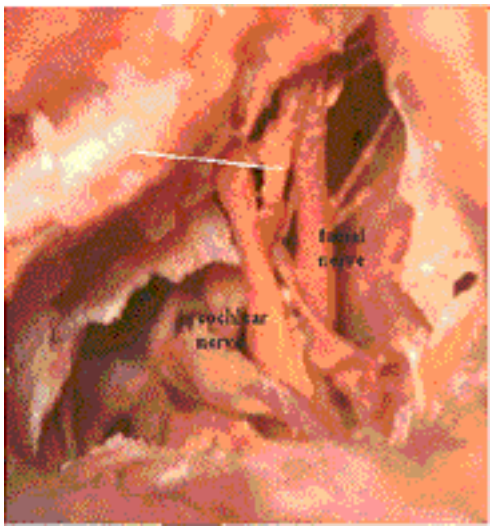

Figure 3 Microscope mounted measuring device to measure the nerve in-situ. The measuring probe was mounted on a x-y-z axis calibrated micromanipulator on a stereotaxic frame. The manipulator and operating microscope were positioned parallel to the length of the nerve to avoid parallax. The nerve was measured at a point that corresponded to the radiological point measured

Table 1.

Specimen	***Side***	***Measurements (mm)***	
		MRI	***Direct***
Head A	*R*	0.98	1.20
	L	0.89	1.33
Head B	*R*	1.15	1.50
	L	0.83	1.16
Head C	*R*	0.69	1.06
	L	1.07	1.18